Critical behavior of the three-dimensional Ising model: A high-resolution Monte Carlo study

Alan M. Ferrenberg and D. P. Landau
Center for Simulational Physics, The University of Georgia, Athens, Georgia 30602
(Received 27 February 1991)

Using recently developed histogram techniques and an ultrafast multispin coding simulation algorithm, we have investigated the critical behavior of the $d=3$ simple-cubic Ising model. We have studied lattice sizes ranging from $L=8$ to 96 using between 3×10^6 and 12×10^6 Monte Carlo steps (complete lattice updates). By accurately measuring the finite-size behavior of several different thermodynamic quantities, we are able to determine the critical properties with a precision comparable to that obtained with Monte Carlo renormalization-group and sophisticated series-expansion techniques. The best estimate of the inverse critical temperature from our analysis is $K_c=0.221\,659\,5\pm0.000\,002\,6$. The advantages of the histogram technique are discussed, as are the potential problems that can arise at this level of resolution.

I. INTRODUCTION

Because of their simplicity, Ising models have served as fertile testing grounds for innumerable projects in statistical mechanics. Although the one- and two-dimensional Ising models have been solved analytically, the three-dimensional model has defied solution in spite of intense effort.[1,2] While the exact behavior is as yet unknown, various numerical methods have succeeded in providing accurate information about the nature of the phase transition. Series-expansion data[3] have been produced and analyzed with increasing sophistication yielding impressive estimates for T_c as well as the critical exponents. Renormalization group and ϵ-expansion studies[4,5] have provided accurate estimates for the exponents. The Monte Carlo renormalization group[6–8] (MCRG) has been used to determine the critical temperature and critical exponents with high accuracy. A recent sophisticated reanalysis of series-expansion data[9] has also yielded an accurate estimate for T_C, but this value appears to be just outside the errors of the MCRG study.

The importance of these studies has been twofold. First, the knowledge gained has provided valuable information about critical exponents, scaling, corrections to scaling, etc., which has helped develop our understanding of the critical properties of the Ising model as well as critical behavior in general. Beyond this, however, accurate numerical estimates of various critical properties provide stringent tests for ascertaining the quality of approximate techniques as well as of supposed exact solutions.

Monte Carlo (MC) simulations have also been used to investigate the $d=3$ Ising model. Early studies[10] applying finite-size scaling analyses produced results of only modest quality due to the limitations (low statistics and small system sizes) imposed by the computers existing at the time. Much longer Monte Carlo runs were made by Barber *et al.* using a special purpose processor,[11] but subsequent work by several groups[12–14] showed that these simulations were in error, presumably because of random-number generator problems.

Performing a high-precision finite-size scaling analysis using standard MC techniques is very difficult due to constraints on the available computer resources. To accurately locate the position of the maximum in a thermodynamic derivative, which defines an effective (finite-lattice) transition temperature $T_c(L)$, one must perform multiple simulations in the vicinity of the peak. (The uncertainty in the location of the peak decreases as the number of simulations is increased.) To reduce the effects of corrections to scaling and finite-size scaling (see Sec. II B), the simulations must be performed on large systems which require more computer time. In addition, each of the multiple simulations must be of high accuracy, which is made more difficult because of critical slowing down near the transition. A further problem is that different thermodynamic derivatives have their peaks at different temperatures so that the process of performing multiple high-precision simulations to locate a peak must be repeated for each quantity considered. Because of this need to obtain high resolution data at many temperatures, standard Monte Carlo simulations have not previously been able to compete with other numerical techniques in providing highly accurate estimates for T_c.

The recent introduction of histogram techniques[15–18] to extract the maximum information from Monte Carlo simulation data at a single temperature enhances the potential resolution of Monte Carlo methods substantially. In this paper we present the results of an extensive Monte Carlo study of the critical behavior of the $d=3$ Ising model. The data were generated using a vectorized multispin coding simulation algorithm and were analyzed using histogram methods together with finite-size scaling techniques to obtain highly accurate estimates for the critical temperature and exponents. An important feature of this study is the analysis of several thermodynamic quantities including the specific heat and susceptibility as well as the fourth-order magnetization cumulant and derivatives and logarithmic derivatives of the magnetization. From this analysis we obtain a comprehensive picture of finite-size effects and the predicted critical behavior in the thermodynamic limit.

II. BACKGROUND

A. Monte Carlo method

We have considered the three-dimensional ferromagnetic Ising model with the Hamiltonian

$$\mathcal{H}=-J\sum_{\langle i,j\rangle}\sigma_i\sigma_j\ . \tag{1}$$

The spins σ_i take on the values ± 1 and the sum goes over all nearest-neighbor pairs. In discussing the critical properties of the Ising model, it is customary to work with the dimensionless coupling constant K related to the interaction constant J by $K=J/k_BT$. We also define the dimensionless energy E as $E=\sum_{\langle i,j\rangle}\sigma_i\sigma_j$.

We have simulated $L\times L\times L$ simple cubic lattices with fully periodic boundary conditions using an efficient vectorized multispin coding algorithm.[19] The system is decomposed into interpenetrating sublattices and up to 64 spins on a single sublattice are packed into a single 64-bit word on the CDC Cyber 205. All spins in a word are "flipped" at once and the entire process is vectorized to increase the speed still further. In this program, a new random number is generated for each spin update. This improves the quality of the data at the expense of a reduction in the speed. (Despite this, the maximum speed of the program is still an impressive 3.8×10^7 spin flip trials per second.) The program produces quasirandom numbers using a vectorized Tausworthe (shift-register) generator.[20–21] We have tested the algorithm for different values of the "magic numbers" ($p=1279$, $q=1063$ and $p=250$, $q=103$) to check for any systematic errors which could be introduced. Within the accuracy of this study no systematic effects were observed. (Results of this test are included in Tables I and II.)

Much of the data used in our analysis had been generated previously for studies of critical relaxation,[22] although additional data were also obtained for several of the system sizes. Most of these simulations were performed at $K=0.221\,654$, an estimate for the critical coupling K_c obtained by MCRG analysis.[6] A few simulations were also performed at other values of K, including couplings much below K_c, to check for systematic errors in the histogram analysis.[23] This will be discussed in detail in Sec. III. Data were obtained for lattices with $8\le L\le 96$, and between 3×10^6 and 1.2×10^7 MCS (complete lattice updates) were performed. Such long runs are necessary to reduce the systematic and statistical errors which arise due to the finite number of samples taken.[24] Measurements were made at intervals of either 5 or 10 MCS after up to 10^5 MCS were discarded for equilibrium. For the largest lattice, the total run length is more than 5000 times the relevant correlation time. A detailed analysis of the correlation times for these simulations has been presented elsewhere.[22] Values of the magnetization and energy were stored as a function of time and were analyzed as described in the next two sections.

B. Finite-size scaling analysis

The critical behavior of a system in the thermodynamic limit may be extracted from the properties of finite systems by examining the size dependence of the singular part of the free energy density. This finite-size scaling approach was first developed by Fisher and has proven to be quite powerful.[25–27]

According to this theory, the free energy of a system of linear dimension L is described by the scaling ansatz

$$F(L,T,h)=L^{-(2-\alpha)/\nu}\mathcal{F}^0(tL^{1/\nu},hL^{(\gamma+\beta)/\nu})\ , \tag{2}$$

where $t=(T-T_c)/T_c$ (T_c is the infinite-lattice critical temperature) and h is the magnetic field. The critical exponents α, β, γ, and ν are all the appropriate values for the infinite system. The various thermodynamic properties can be determined from Eq. (2) and have corresponding scaling forms, e.g.,

$$m=L^{-\beta/\nu}\mathcal{X}^0(x_t)\ , \tag{3}$$

$$C=L^{\alpha/\nu}\mathcal{Z}^0(x_t)\ , \tag{4}$$

where $x_t=tL^{1/\nu}$ is the temperature scaling variable. Because we will be interested only in zero-field properties, x_t is the only relevant thermodynamic variable.

In this study we wish to determine the transition temperature accurately. This is accomplished by finding the location of the peak in a thermodynamic derivative, for example the specific heat. For a finite lattice the peak occurs at the temperature where the scaling function $\mathcal{Z}^0(x_t)$ is maximum, i.e., when

TABLE I. Estimates for $K_c(L)$, for $L=16$, obtained from various derivatives. The values of K shown at the top give the couplings at which the simulations were made. The values of RNG refer to the two different pairs of shift-register random number generator "magic numbers" used.

	$K=0.221\,654$ RNG=1	$K=0221\,654$ RNG=2	$K=0.221\,500$ RNG=2
$\lvert m\rvert$	0.222 193 4(68)	0.222 180 3(30)	0.222 183 0(79)
χ	0.221 810 8(66)	0.221 804 2(58)	0.221 807 2(50)
$\ln\lvert m\rvert$	0.221 566 8(82)	0.221 562 5(80)	0.221 554 2(50)
$\ln m^2$	0.221 447 4(91)	0.221 462 5(60)	0.221 473(10)
U	0.221 271(14)	0.221 262 5(92)	0.221 266 1(60)

TABLE II. Maximum values of derivatives obtained from three different simulations. The values of K shown at the top give the couplings at which the simulations were performed. The values of RNG refer to the two different pairs of shift-register random number generator "magic numbers" used.

	$K=0.221\,654$ RNG=1	$K=0.221\,654$ RNG=2	$K=0.221\,500$ RNG=2
$\lvert m\rvert$	97.71(46)	97.41(42)	97.73(49)
χ	58.50(30)	58.47(36)	58.52(22)
$\ln\lvert m\rvert$	470.1(26)	471.1(18)	471.7(32)
$\ln m^2$	788.7(40)	791.0(47)	790.2(25)
U	183.7(22)	185.9(32)	184.3(17)

$$\left.\frac{dZ^0(x_t)}{dx_t}\right|_{x_t=x_t^*}=0\ . \tag{5}$$

This temperature is the finite-lattice (or effective) transition temperature $T_c(L)$, defined through the condition $x_t=x_t^*$ to vary with the lattice size, asymptotically, as

$$T_c(L)=T_c+T_c x_t^* L^{-1/\nu}\ . \tag{6}$$

These results for the scaling of thermodynamic quantities and $T_c(L)$ are valid only for sufficiently large L and temperatures close to T_c. For smaller systems, corrections to finite-size scaling must be taken into account. These manifest themselves as power-law corrections with an exponent $-w$ so that, for example, the magnetization at T_c would scale with system size like $L^{-\beta/\nu}(1+cL^{-w})$. As we move away from T_c, corrections to scaling due to irrelevant scaling fields,[28] or nonlinearities in the scaling variables[29] must be taken into account. Corrections due to irrelevant fields are expressed in terms of an exponent θ leading to additional terms like $a_1t^{\theta}+a_2t^{2\theta}+\cdots$ while nonlinearities in the scaling variables give rise to correction terms like $b_1t^1+b_2t^2+\cdots$. The temperatures we consider in the analysis differ from T_c (or $t=0$) by amounts proportional to $L^{-1/\nu}$ [Eq. (6)] so that the correction to scaling terms at these temperatures can be expressed by power-law corrections of the form $a_1L^{-\theta/\nu}+\cdots$ and $b_1L^{-1/\nu}+\cdots$. Fully taking into account these corrections to scaling and to finite-size scaling is complicated by two factors.

(1) The value of the correction exponent has been estimated to be $\theta\simeq 0.5$ (Refs. 30 and 31) so that the exponents $2\theta/\nu$ and $1/\nu$ may be very similar, but still different enough that a single correction term will not compensate for both of them. Also the amplitude of the first correction $L^{-\theta/\nu}$ may be zero for some thermodynamic quantities but not for others.

(2) Each correction term we consider requires two parameters in a fit, which decreases the number of degrees of freedom. Including more than one independent correction term is nearly impossible, even with high-quality data.

For these reasons, we fit our data with at most a single correction term, $L^{-\omega}$, in the hope that (1) our system sizes are large enough that any corrections will be small and (2) that any residual corrections from more than one term can be well approximated by a single correction. A second possibility is to assume that away from T_c the corrections to scaling are more important than the corrections to finite-size scaling and then make use of the theoretical predictions and fit the data with two correction terms $L^{-\theta/\nu}$ and $L^{-1/\nu}$. We will compare these two approaches in Sec. IV.

If we take the correction term into account, the estimate for $T_c(L)$ is then modified to be

$$T_c(L)=T_c+\lambda' L^{-1/\nu}(1+b'L^{-\omega}) \tag{7}$$

or, in terms of the coupling K

$$K_c(L)=K_c+\lambda L^{-1/\nu}(1+bL^{-\omega})\ . \tag{8}$$

Because each thermodynamic function has its own scaling function, the value of x_t^*, and therefore λ, depends, in magnitude and sign, on the particular function measured. For example, for the $d=3$ Ising model, the location of the specific heat maximum occurs further away from (above) K_c than the location of the maximum of the magnetic susceptibility. [Estimates for $K_c(L)$ from other quantities approach K_c from below so that rough upper and lower bounds on K_c can be determined by looking at the values of $K_c(L)$ for the largest lattice.] However, before Eq. (8) can be used to determine K_c, it is necessary to have both an accurate estimate for ν and accurate values for $K_c(L)$.

It has traditionally been difficult to determine ν from Monte Carlo simulation data because of a lack of quantities which provide a direct measurement. This situation was greatly improved by Binder's[32] introduction of the fourth-order magnetization cumulant U defined by

$$U=1-\frac{\langle m^4\rangle}{3\langle m^2\rangle^2}\ , \tag{9}$$

where $m=L^{-d}\sum_i\sigma_i$ is the magnetization per spin. Binder showed that the slope of the cumulant at K_c, or anywhere in the finite-size scaling region, varies with system size like $L^{1/\nu}$. In particular, the maximum value of the slope scales as $L^{1/\nu}$. If we take into account a correction to scaling term, the size dependence of the peak becomes

$$\left.\frac{dU}{dK}\right|_{\max} = aL^{1/\nu}(1+bL^{-\omega}) . \tag{10}$$

(Note that other quantities such as the specific heat and magnetic susceptibility diverge with different powers). The location of the maximum slope of U also serves as an estimate for an effective transition coupling which can be used to determine K_c. Because of these properties, the cumulant is an important part of our analysis. In the same paper, Binder[32] introduced the "cumulant crossing" method which extracts a transition temperature by examining the behavior of the magnetization cumulant for different lattice sizes. We will discuss this method of determining K_c in Sec. IV E.

C. Thermodynamic derivatives

Additional estimates for ν can also be obtained by considering less traditional quantities which should nonetheless possess the same critical properties. For example, the logarithmic derivative of any power of the magnetization

$$\frac{\partial}{\partial K}\ln\langle m^n\rangle = \frac{1}{\langle m^n\rangle}\frac{\partial}{\partial K}\langle m^n\rangle = \left[\frac{\langle m^n E\rangle}{\langle m^n\rangle} - \langle E\rangle\right] , \tag{11}$$

has the same scaling properties as the cumulant slope. The location of the maximum slope also provides us with an additional $K_c(L)$. In our analysis we will consider the logarithmic derivatives of $\langle |m| \rangle$ and $\langle m^2 \rangle$, as well as the derivative of the cumulant, to determine ν.

Once ν has been calculated, it is necessary to determine estimates for $K_c(L)$. In addition to the values for the effective transition coupling we obtain from these three quantities, we also determine $K_c(L)$ from the specific heat, Eq. (12a), the derivative of $|m|$ with respect to K, Eq. (12b), and the finite-lattice susceptibility, Eq. (12c):

$$C = K^2 L^{-d}(\langle E^2\rangle - \langle E\rangle^2) , \tag{12a}$$

$$\frac{\partial\langle |m| \rangle}{\partial K} = (\langle |m|E\rangle - \langle |m|\rangle\langle E\rangle) , \tag{12b}$$

$$\chi' = KL^d(\langle |m|^2\rangle - \langle |m|\rangle^2) . \tag{12c}$$

The derivative with respect to K of a thermodynamic quantity of interest is calculated using the cross-correlation of that quantity with the energy E as in Eqs. (12a) and (12b) above. The true susceptibility calculated from the variance of m, $\chi = KL^d(\langle m^2\rangle - \langle m\rangle^2)$, cannot be used to determine $K_c(L)$ because it has no peak. For short Monte Carlo runs $\langle m \rangle$ is nonzero below $T_c(L)$, but for sufficiently long runs any finite system oscillates between states with positive and negative magnetization which leads to $\langle m \rangle \simeq 0$. Therefore, any peak in χ is merely due to the finite statistics of the simulation.

III. HISTOGRAM METHOD

A. Theory

The idea of using histograms to increase the amount of information obtained from Monte Carlo simulations has been around for more than 30 years but has only recently been applied with success to the study of critical phenomena.[15–18] The histogram technique used in our analysis has been described in detail elsewhere.[17] Here we provide a brief description of the method as implemented in this study.

A Monte Carlo simulation performed at $T = T_0$ generates system configurations with a frequency proportional to the Boltzmann weight, $\exp[-\beta_0 \mathcal{H}]$, where $\beta_0 = 1/k_B T_0$, and $\mathcal{H}$ is the Hamiltonian of the system being studied. As mentioned in Sec. II, we wish to consider the $d = 3$ nearest-neighbor Ising model with the Hamiltonian given by Eq. (1). For a simulation at temperature T_0, corresponding to coupling K_0, the Boltzmann weight can be expressed as $\exp[K_0 E]$. The probability of simultaneously observing the system with (dimensionless) energy E and magnetization $M = \sum_i \sigma_i$ is then

$$P_{K_0}(E,M) = \frac{1}{Z(K_0)} W(E,M)\exp[K_0 E] , \tag{13}$$

where $W(E,M)$ is the number of configurations (density of states) with energy E and magnetization M, and $Z(K_0)$ is the partition function of the system. Because the simulation generates configurations according to the equilibrium probability distribution, a histogram $H(E,M)$ of E and M kept during the simulation provides an estimate for the equilibrium probability distribution, becoming exact in the limit of an infinite-length run. For a finite-length simulation, the histogram will suffer from statistical errors, but $H(E,M)/N$, where N is the number of measurements made, still provides an estimate for $P_{K_0}(E,M)$ over the range of E and M values generated during the simulation. Keeping this in mind we modify Eq. (13) to read

$$H(E,M) = \frac{N}{Z(K_0)} \tilde{W}(E,M)\exp[K_0 E] , \tag{14}$$

where $\tilde{W}(E,M)$ is an estimate for the true density of states $W(E,M)$. From the form of Eqs. (13) and (14), it is simple to see that knowledge of the distribution at one value of K is sufficient to determine it for any K. To see this, recall that the probability distribution for any value of K has the same form as Eq. (13):

$$P_K(E,M) = \frac{1}{Z(K)} W(E,M)\exp[KE] . \tag{15}$$

Next, note that because we know the distribution at K_0, from the histogram $H(E,M)$, we can invert Eq. (14) to determine $\tilde{W}(E,M)$:

$$\tilde{W}(E,M) = \frac{Z(K_0)}{N} H(E,M)\exp[-K_0 E] . \tag{16}$$

If we now replace $W(E,M)$ in Eq. (15) with the expression for $\tilde{W}(E,M)$ from Eq. (16), and normalize the distri-

bution, we find that the relationship between the histogram measured at $K=K_0$ and the (estimated) probability distribution for arbitrary K is

$$P_K(E,M)=\frac{H(E,M)\exp[\Delta KE]}{\sum_{E,M} H(E,M)\exp[\Delta KE]} , \tag{17}$$

with $\Delta K=(K-K_0)$. From $P_K(E,M)$, the average value of any function of E and M, $f(E,M)$, can be calculated as a continuous function of K

$$\langle f(E,M)\rangle_K=\sum_{E,M} f(E,M)P_K(E,M) . \tag{18}$$

Equations (17) and (18) will be referred to as the *single-histogram equations.*

The ability to continuously vary K makes the histogram method ideal for locating the peak in a thermodynamic derivative. Using Eq. (18) we can calculate the average value of a thermodynamic quantity as well as any order derivative of the quantity with respect to K. For example, the derivative of $\langle|m|\rangle$ with respect to K was given in Eq. (12b) and the second derivative is then simply

$$\frac{\partial^2\langle|m|\rangle_K}{\partial K^2}=(\langle|m|E^2\rangle_K-\langle|m|\rangle_K\langle E^2\rangle_K) -2\langle E\rangle_K\frac{\partial\langle|m|\rangle_K}{\partial K} . \tag{19}$$

Higher order derivatives can also be calculated if needed. When a function, such as the specific heat, is maximum, its derivative with respect to K is zero. The problem of locating a peak can therefore be turned into that of finding the root of a function. This can be accomplished, for example, by using Newton's method since any derivative can be calculated, in terms of cross-correlations with the energy E, as a continuous function of K as described above. This process can be automated so that peaks in functions can be located quickly and with high accuracy.

B. Implementation of the histogram method

Because of the finite length of the MC run, the single-histogram equations provide reliable results only for a relatively narrow range of K values around K_0. As K is varied, the peak in the distribution calculated using Eq. (17) moves away from that of the measured histogram. When K differs too much from K_0, the peak is shifted into the "wings" of the measured histogram where the statistical uncertainty is high. This causes increased statistical errors in the calculated distribution and can lead to unreliable results. To demonstrate this effect in Fig. 1 we plot the normalized (total) energy histogram for the $L=16$ lattice measured at $K=0.221\,654$ (1.2×10^7 MCS sampled every 10 MCS) along with the probability distributions for two additional couplings ($K=0.224$ and $K=0.228$) calculated from this histogram using the single-histogram equation Eq. (17). The calculated distribution for $K=0.224$ is fairly smooth, although the high-energy side of the distribution, which occurs closer to the peak of the measured histogram, is clearly smoother than the low-energy side. The "thickening" of the distribution arising from the tail of the measured histogram is an indication that the statistical errors are beginning to be amplified and that the extrapolation is therefore close to its limit of reliability. The distribution calculated for $K=0.228$ clearly suffers from the amplification of the errors in the wing and would not provide reliable results. This limitation in ΔK must always be kept in mind, particularly for large systems because the reliable range of K values decreases as the system size increases.[17]

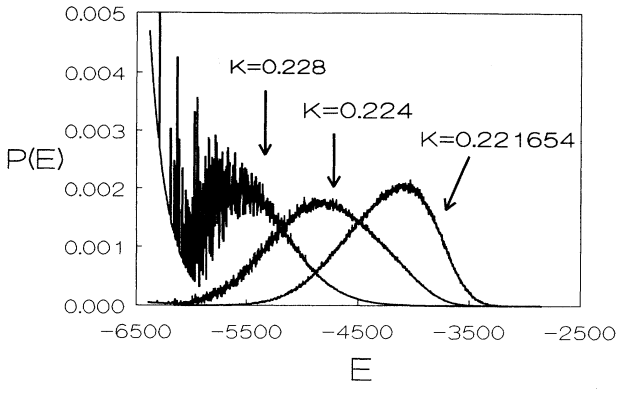

FIG. 1. Probability distribution for the (unnormalized) energy for $L=16$ plotted vs dimensionless energy E. The data from the simulation are labeled by the coupling at which the simulation was carried out, $K=0.221\,654$. The other distributions were produced by the reweighting technique described in the text.

In addition to this amplification of statistical errors, the single-histogram method can also suffer from *systematic* errors[23] if $|\Delta K|$ is too large. This again results from the finite length of the simulation. While the exact distribution has values for every possible system energy, the histogram generated in a finite simulation contains entries for only a range of energies. We demonstrate this effect in Fig. 2, again using the measured energy histogram for the $L=16$ lattice. In Fig. 2 we show the distribution measured at $K=0.221\,654$ as a function of the dimensionless energy per spin $\mathcal{E}$. In the same figure we plot the average energy/spin, calculated using Eq. (18), plotted versus K. For large K, the average energy per spin approaches the value $\mathcal{E}\simeq-1.50$ although the correct $K\to\infty$ value is $\mathcal{E}=-3.0$. Similarly, for $K\to0$ the calculated energy per spin approaches $\mathcal{E}=-0.75$ although the correct result is $\mathcal{E}=0.0$. This behavior demonstrates one kind of systematic error present in the histogram method. For ΔK large and positive the average value of the energy will be systematically overestimated while for large negative ΔK, the average of $\mathcal{E}$ will be systematically underestimated. Figure 2 is also interesting because it points out the relationship between K and $\mathcal{E}$ (or E). Because the partition function $Z(K)$ is the Laplace transform of the

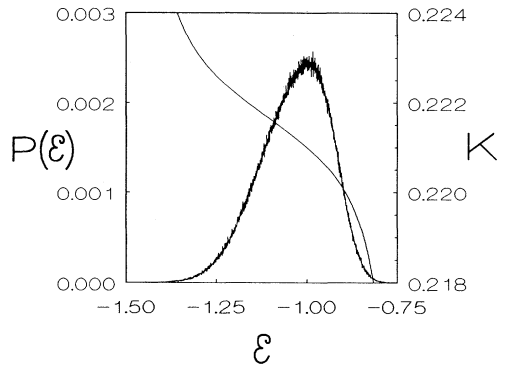

FIG. 2. Probability distribution for the (normalized) energy for $L=16$ (left scale) and the computed (dimensionless) energy-coupling relation (right scale). The simulation was performed at $K=0.221\,654$.

density of states $W(\mathcal{E})$, K and $\mathcal{E}$ are conjugate variables. We can make use of this relationship in a plot like Fig. 2 to estimate the range of reliable K values. The region of energies near the peak of $P(\mathcal{E})$, say from $\mathcal{E}=-1.3$ to $\mathcal{E}=-0.8$, map onto a corresponding region of K values, from $K=0.218$ to $K=0.223$ as shown in Fig. 2. Because the relative statistical error in the histogram over this range of $\mathcal{E}$ values is small, we expect that quantities calculated over the corresponding range of K values will be reliable.

By performing a small number of additional simulations at different values of K we can guarantee that the results obtained from the single-histogram equation applied to data generated at the initial K do not suffer from systematic errors. To check for systematic errors in the histogram analysis we performed additional simulations for $L=32$ at $K=0.2215$ and determined the location and value of the peaks in the thermodynamic derivatives used in our analysis. Simulations were also performed using two different sets of the random number generator "magic numbers." Table I compares our determination of the location of the peaks for five different quantities: the derivatives (with respect to K) of $|m|$ and U, the logarithmic derivatives of $|m|$ and m^2, and the finite lattice susceptibility χ'. Table II compares the values of the peaks for the five quantities. Within the observed statistical errors, no systematic deviations are present. To further test for systematic errors, we can use the histogram measured at $K=0.221\,654$ to predict the behavior of the system at $K=0.2215$ then compare the results with those obtained directly from the simulation performed at $K=0.2215$. The reweighted results agreed, within the calculated error (±1 standard deviation), with the directly measured results for all quantities except the specific heat. (However, the specific heats did agree within $\pm2\sigma$.)

An additional problem which arises for large systems is that it becomes impossible to fit the histogram in the computer's memory. Because both E and M are extensive variables, the amount of memory required to store the histogram increases like the square of the volume of the system (the complete histogram for our largest lattice, $L=96$, would require nearly 10^7 megabytes of computer memory). Fortunately the solution to the problem is fairly straightforward. In our analysis we need to calculate the average of three functions of the magnetization per spin, $|m|$, m^2, and m^4, as well as several mixed functions like $E^n m^2$. Using Eq. (18), the average of such a function is given by

$$\langle E^n f(m)\rangle_K=\frac{\sum_{E,M} E^n f(m)H(E,M)\exp[\Delta KE]}{\sum_{E,M} H(E,M)\exp[\Delta KE]}\ . \tag{20}$$

By performing the sums over M first, this average can be reexpressed as

$$\langle E^n f(m)\rangle_K=\frac{\sum_{E} E^n\langle f\rangle(E)H(E)\exp[\Delta KE]}{\sum_{E} H(E)\exp[\Delta KE]}\ , \tag{21}$$

where $H(E)=\sum_M H(E,M)$ is the energy histogram and $\langle f\rangle(E)$ is the constant-energy average of $f(m)$ estimated from the simulation data. This reduces the calculation to a one-dimensional problem. We therefore use the simulation data to construct the one-dimensional histogram $H(E)$ as well as three constant-E averages: $\langle|m|\rangle(E)$, $\langle m^2\rangle(E)$, and $\langle m^4\rangle(E)$. From these four one-dimensional arrays we can calculate all of the thermodynamic quantities needed for our analysis.

IV. RESULTS

A. Data and error analysis

To estimate the errors in our results, we first divided each simulation into a set of statistical samples (bins), (between 5 and 11 bins were used), then calculated all quantities of interest for each of the bins. Estimates for the statistical error were then determined by considering the distribution of values obtained from each bin. Error bars are given as $\pm1\sigma$ where σ is the standard deviation of the mean taken over all of the bin values. (This procedure is exactly that used to estimate errors in standard Monte Carlo studies.) Because each histogram is used to determine multiple quantities, some correlations are expected between the different results. We find, however, that such correlation effects are smaller than the statistical errors, and in our judgment the individual errors may be treated as uncorrelated. To test the effect of systematic errors[24] (underestimation of response functions), we performed our analysis for bins of different sizes choosing the final bin sizes so that systematic errors were negligible compared to the statistical error. An additional check for possible numerical error was made by repeating some of the histogram analysis using double precision arithmetic (128 bits on the Cyber 205). No change was observed within the first 10 significant digits. In Fig. 3 we

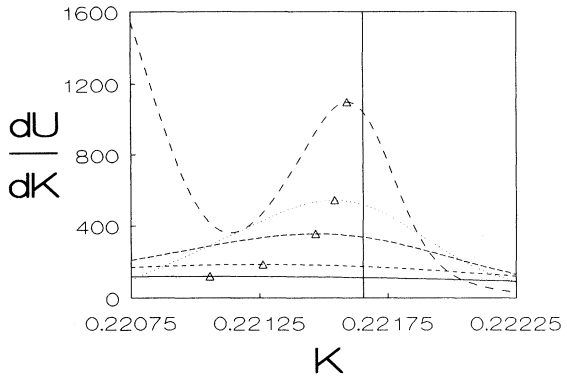

FIG. 3. The derivative of the magnetization cumulant, calculated using Eq. (18), is plotted as a function of K for $L=24$, 32, 48, 64, and 96. The triangles represent the location of the peaks. In all cases the error in the peak value is smaller than the symbol. The increase in dU/dK for small K ($L=96$) is nonphysical and results because these K values are outside the range of validity for $L=96$ (see Sec. III B). The location of the simulated coupling is marked by a vertical line.

plot the derivative of the magnetization cumulant, calculated using the single-histogram method, for $L \geq 24$. The simulated value of K is shown by a vertical line and the triangles mark the location of the peak for each lattice size. (The error in the peak value is smaller than the size of the triangle for every system size.) The breakdown of the single-histogram method can clearly be seen for the $L=96$ curve. The increase in dU/dK for $K \simeq 0.2208$ is nonphysical and occurs only because these values of K are well beyond the range of validity for $L=96$. (For lower K values the slope even becomes negative.) Other thermodynamic derivatives showed quite similar qualitative behavior and the data are thus not shown.

B. Finite-size scaling analysis to determine ν

The critical exponent ν can be estimated without any consideration of the critical coupling K_c. As stated in Sec. II, we can extract ν by considering the scaling behavior of certain thermodynamic derivatives, for example, the derivative of the magnetization cumulant and the logarithmic derivatives of $|m|$ and m^2. In Fig. 4 we plot the maximum value of these derivatives as a function of system size on a log-log scale. For sufficiently large systems we should be able to ignore the correction term so that linear fits of the logarithm of the derivatives as a function of $\ln L$ provide estimates for $1/\nu$. To verify that our system sizes are large enough to justify this approximation, we performed several linear fits using system sizes $L_{\min} \leq L \leq 96$, each time choosing a smaller value for $L_{\min}$. We find that $L_{\min}=24$ is the smallest value we can use except in the case of the derivative of the magnetization cumulant where linear fits are still satisfactory for $L_{\min}=12$. The results for $1/\nu$ from these fits are given in Table III. Combining these three estimates we obtain $1/\nu=1.594\pm0.004$ or $\nu=0.627\pm0.002$.

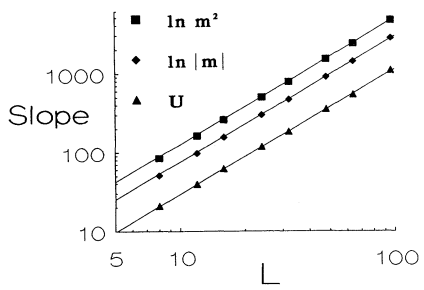

FIG. 4. Log-log plot of the size dependence of the maximum values of derivatives of various thermodynamic quantities used to determine ν. The straight lines (with slopes corresponding to $\nu=0.6289$) show the asymptotic behavior of the fits.

TABLE III. Estimates for $1/\nu$ obtained by finite-size scaling of the maxima of the cumulant slope and the logarithmic derivatives of m^2 and $|m|$.

	$1/\nu$
U	1.5887±0.0085
$\log m^2$	1.5970±0.0061
$\log\|m\|$	1.5958±0.0067

By including a correction term, see Eq. (10), we are able to incorporate the data from smaller systems. Rather than performing nonlinear fits to include this term, we choose to take the corrections into account in the following manner. We fit the derivatives to Eq. (10) by fixing the values of ν and ω, determining the values of a and b which minimize the χ^2 of the fit, and then repeated the procedure for different values of ν and ω. (This approach effectively linearizes the fit at the expense of giving up individual error estimates for ν and ω.) By scanning over a region of (ν,ω) space, we determined the global minimum in χ^2 and found $1/\nu=1.590\pm0.002$ or $\nu=0.6289\pm0.0008$. The correction term for the cumulant is so small that we cannot obtain a reliable estimate for the correction exponent. However, for the logarithmic derivatives of $|m|$ and m^2 the correction exponent is consistent with $\omega \sim 1$ which falls almost exactly between θ/ν and $1/\nu$ for $\theta=0.5$. We therefore suspect that our "effective" exponent is indeed compensating for both of these corrections. This point will be discussed further in Sec. IV D.

C. Finite-size scaling analysis to determine K_c

With ν determined quite accurately we are now in position to estimate K_c. As discussed in Sec. II, the location of the maxima of various thermodynamic derivatives provide estimates for effective transition couplings $K_c(L)$ which scale with system size like Eq. (8). We plot these estimates for $K_c(L)$ as a function of $L^{-1/\nu}$ for $L=12$, 16,

24, 32, 48, 64, and 96 in Fig. 5. The lines are fits of the data to Eq. (8) with $\nu=0.6289$. Before proceeding with the analysis, we first applied the criterion discussed in Sec. III B to verify that our results did not suffer from statistical and systematic errors due to the histogram reweighting procedure. We found that the specific heat peaks (open circles in Fig. 5), which occur further from the simulated temperature than any other quantity considered here, fall just outside the range of validity of the histogram analysis, especially for $L=96$. Because of this, the calculated errors for the specific heat are smaller than the actual deviation from the correct finite lattice behavior. We can compensate for this systematic underestimation of the error, particularly pronounced for $L=96$, by either increasing the error values, or by removing the $L=96$ result. In either case, we find that the estimate for K_c, is in agreement with that determined from the other quantities, but the final uncertainty is much larger. The result for the derivative of $|m|$ on the $L=96$ system is, in our opinion, just at the limit of reliability for the histogram analysis. There is a noticeable curvature in the lines in Fig. 5 indicating that corrections to scaling are important for the smaller systems. In Fig. 6 we show a magnification of Fig. 5, using only the results for $L\geq 24$ and excluding the specific heat. The solid lines here are linear fits to Eq. (8) with no correction term and ν fixed to the value calculated above. There are no obvious systematic derivation from the straight lines in this plot.

As noted in Sec. II B, analyzing several estimates for $K_c(L)$ has the advantage that rough bounds on K_c can be determined by looking at the estimates for $K_c(L)$ for the largest system without performing fits to Eq. (8). By considering only the two quantities which approach K_c with the smallest slopes, the finite-lattice susceptibility from above and the logarithmic derivative of $|m|$ from below we would conclude that $K_c=0.221\,67\pm0.000\,02$. To further increase the accuracy, however, it is necessary to perform the extrapolation to infinite system size using Eq. (8). For sufficiently large L, $K_c(L)$ should extrapolate linearly with $L^{-1/\nu}$ to K_c; however, as seen in Fig. 5 there is a noticeable curvature for small system sizes. We can take the corrections into account as described above for the determination of ν. This procedure provides us with estimates for ω and K_c for each of the quantities we consider and these values are given in Table IV.

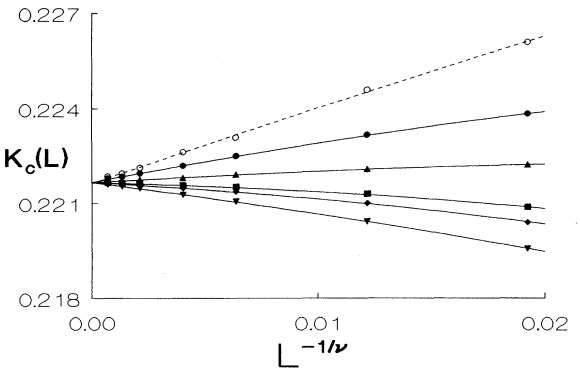

FIG. 5. Size dependence of the finite-lattice effective critical temperatures estimated from several quantities for $L=12$, 116, 24, 32, 48, 64, and 96. The open circles represent the data for the specific heat while the other symbols are explained in Fig. 6. The lines (dashed for the specific heat and solid for the other quantities) are fits to Eq. (8) with $\nu=0.6289$ and including the correction term.

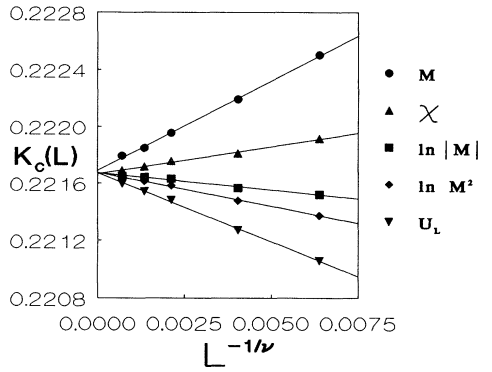

FIG. 6. Magnification of Fig. 5 using the data for $L\geq 24$ and excluding the specific heat. The curves are straight-line fits to Eq. (8) with $\nu=0.6289$ and no correction term.

Combining these estimates we find a final value $K_c=0.221\,659\,5\pm0.000\,002\,6$. The values of the correction exponent are again consistent with $\omega\simeq 1$ except for the finite-lattice susceptibility (which has the smallest correction term). We can also perform this kind of fit by allowing both ω and ν to vary. This approach yields consistent estimates for ν and K_c but with larger errors due to the reduced number of degrees of freedom of the fit.

Based on a suggestion by Fisher,[33] we also attempted to perform our fits by replacing the system size L with $L+l_0$ where l_0 is an extrapolation length appropriate for free or fixed boundary conditions. Although our systems had fully periodic boundary conditions we incorporated this suggestion in the analysis because including l_0 in a fit may effectively compensate for additional finite lattice corrections. However, to leading order, including l_0 pro-

TABLE IV. Values of the critical coupling K_c and correction exponent ω obtained by finite-size scaling of locations of the peaks of thermodynamic derivatives.

	ω	K_c
$\lvert m\rvert$	0.976	0.221 667 0±0.000 007 2
χ'	0.258	0.221 654 9±0.000 005 2
$\ln\lvert m\rvert$	1.053	0.221 659 7±0.000 004 9
$\ln m^2$	1.099	0.221 660 4±0.000 005 3
U	0.812	0.221 655 5±0.000 006 1

vides a correction which goes as L^{-1}. Because this coincides with our estimate for the correction exponent ($\omega \simeq 1$), any further consequence of adding l_0 would be a second-order effect. We found that in some cases, the χ^2 of the fit did decrease slightly for small l_0 ($l_0 \simeq 0.5$) but the estimates for K_c and ν were not affected within the statistical errors.

D. Estimates for ν and K_c using the predicted form for the correction terms

In Sec. II, we stated that a second approach to including the correction to scaling terms would be to assume the theoretical form for the correction and fit quantities, for example, the maximum cumulant slope, to the form

$$\left.\frac{dU}{dK}\right|_{\max} = aL^{1/\nu}(1+bL^{-1/2\nu}+cL^{-1/\nu}) \tag{22}$$

assuming $\theta = 0.5$. Estimates for $K_c(L)$ would then be fit to

$$K_c(L) = K_c + aL^{-1/\nu}(1+bL^{-1/2\nu}+cL^{-1/\nu}) \ . \tag{23}$$

The fact that our single "effective" correction exponent seems to fall between $1/2\nu$ and $1/\nu$ would make a correction of this form plausible. We therefore repeated our finite-size scaling analysis using Eqs. (22) and (23). The reanalysis of thermodynamic derivatives of Sec. IV B provides us with the estimate $1/\nu = 1.5887 \pm 0.0004$ or $\nu = 0.6294 \pm 0.0002$. While we are encouraged by the small statistical error in these values, we believe that this is very fortuitous. The χ^2 of the fit, as a function of $1/\nu$, has a broad shallow minimum so that the actual statistical error, calculated by performing a true nonlinear fit would be larger. Unfortunately we have neither the resolution nor enough different lattice sizes to attempt such a fit. Using this value of ν we then calculated estimates for K_c from Eq. (23). Our result from this analysis is $K_c = 0.221\,657\,4 \pm 0.000\,001\,8$ which is in excellent agreement with our previous estimate. Again, we are encouraged by this result, but until we have sufficient data to resolve two independent correction terms we are more confident with the value presented in Sec. IV C.

E. Phenomenological renormalization of the magnetization cumulant

Estimates for K_c can also be obtained by considering Binder's cumulant crossing technique.[32] In this approach, the magnetization cumulants, Eq. (9), for different lattice sizes are plotted as a function of K and the intersections are determined as a function of the two lattice sizes L and L'. The K value at which the cumulant intersect varies with L and L' as[32]

$$K_{\text{cross}}(L,b) = K_c + gL^{-(w+1/\nu)}\left[\frac{b^{-w}-1}{b^{1/\nu}-1}\right] , \tag{24}$$

where L is the size of the smaller lattice, b is the ratio of lattice sizes (L'/L), and w is a correction to finite-size scaling exponent. In the usual implementation of this technique, ignoring the correction term b^{-w}, one approximates the term $(b^{1/\nu}-1)$ by $(1/\nu)\ln b$, which is valid for *small* b. For fixed L, plots of $K_{\text{cross}}(L,b)$ versus $1/\ln b$ should then extrapolate linearly to K_c as $1/\ln b \to 0$. However, for the system sizes we examined the values of b were too large for this approximation to be valid. Instead, we took a different approach by considering Eq. (24) for fixed b rather than fixed L so that the values of $K_{\text{cross}}(L,b)$ should extrapolate to K_c like $L^{-(w+1/\nu)}$. For the lattice sizes used in our analysis, the approach to K_c was so rapid that we were unable to extract an estimate for w. We also found that the statistical uncertainty in determining the intersections was three to four times larger than that in locating the peaks as in the previous analysis. Keeping this in mind, the estimate for K_c we found by this analysis is $0.221\,66 \pm 0.000\,01$ which agrees with the result obtained above, but is clearly inferior in resolution.

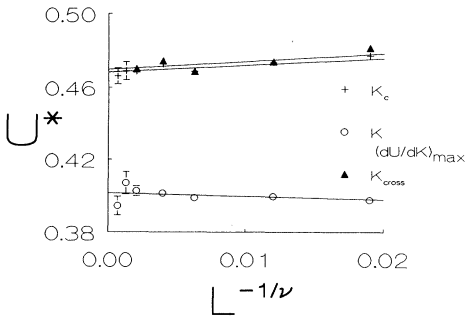

FIG. 7. Size dependence of the reduced fourth-order cumulant obtained for K_c, $K = K_{dU/dK|_{\max}}$ and via cumulant crossing.

The value of the magnetization cumulant at the transition temperature, U^*, is an important universal quantity. We have attempted to extract U^* in three ways; by determining the value of U where the slope of $U(K)$ is maximum, by fixing K at our estimate for K_c and looking at the cumulant there, and by considering the values of $U[K_{\text{cross}}(L,b)]$ for $b=2$ from above. The values of U we obtain by these approaches are shown plotted versus $L^{-1/\nu}$ in Fig. 7. The estimates obtained via cumulant crossings and by considering U at K_c are consistent with each other and suggest $U^* \simeq 0.47$. The value obtained by looking at the value of U where dU/dK is maximum is not consistent with this estimate but rather suggests $U^* \simeq 0.40$. Due to the singular nature of the cumulant as $L \to \infty$, this behavior is not unexpected, and the correct estimates are those calculated at $K = K_c$ and by cumulant crossings.[34]

F. Estimates of other exponents using finite-size scaling

We can also use finite-size scaling to estimate the exponents ν, β/ν, and γ/ν from bulk properties at K_c. The

value of ν which we obtain by looking at the derivative of the magnetization cumulant and the logarithmic derivatives of $|m|$ and m^2 at K_c is identical to that obtained by scaling the maximum value of the derivatives. By determining the scaling behavior of $|m|$ at K_c, we estimate $\beta/\nu=0.518\pm0.007$. (The linear fit for $L\geq 24$ yields $\beta/\nu=0.505$.) Combining this value for β/ν with our estimate for ν, we estimate the exponent β to be $\beta=0.3258\pm0.0044$ which agrees with the ϵ-expansion result 0.3270 ± 0.0015.[5] We can determine γ/ν in two ways. First, we can consider the scaling behavior of the finite-lattice susceptibility defined in Eq. (11c). The analysis of this quantity yields $\gamma/\nu=1.9828\pm0.0057$ or $\gamma=1.2470\pm0.0039$. We can also look at the true susceptibility $\chi=KL^d(\langle m^2\rangle-\langle m\rangle^2)$ at K_c. Analyzing χ at K_c yields $\gamma/\nu=1.970\pm0.011$ or $\gamma=1.2390\pm0.0071$. This estimate for γ is in excellent agreement with the ϵ-expansion value $\gamma=1.2390\pm0.0025$.[5]

G. Discussion

In this section we compare our values of ν and K_c with those obtained by other numerical methods. In Fig. 8 we show the results of our Monte Carlo study as well as other high-resolution simultaneous estimates for ν and K_c.[6–9,18,35] The boxes represent the quoted error bars in both K_c and ν assuming independent errors. (For the results of Ref. 18, only half of the error box is shown because of the large uncertainty in K_c.) The two boxes for Ref. 9 correspond to different choices for the susceptibility exponent γ in the series analysis. To the best of our knowledge, all error estimates represent ±1 standard deviation. Also shown are two estimates for ν only, one from ϵ expansion[5] (which provides no estimate for K_c) and another recent series expansion estimate.[30] The results from our Monte Carlo study are represented by the cross-hatched box. The circles give the reference number where the corresponding values can be found.

Our estimate $\nu=0.6289\pm0.0008$ is in excellent agreement with recent MCRG results of Blöte and co-workers,[7,8] as well as older MCRG work from Pawley and co-workers.[6] The agreement with the histogram Monte Carlo results of Alves, Berg, and Villanova[18] is also good. Our value is also consistent with the ϵ-expansion result of LeGuillou and Zinn-Justin[5] and the series expansion results of Nickel and Rehr[30] and Adler.[35] Transfer matrix Monte Carlo results by Nightingale and Blöte[36] yield $\nu=0.631$ with errors of either 0.006 or 0.002 depending on the range of sizes considered in the analysis. Novotny[37] has recently determined a numerical lower bound on ν in a transfer matrix study of the $d=3$ Ising model. His lower bound, $\nu=0.6302$, lies outside of our estimated error bars, but falls within 2σ of our result. However, our estimate appears to be inconsistent with the Liu and Fisher[9] series expansion results. The estimate for K_c determined in our analysis, $K_c=0.221\,659\,5\pm0.000\,002\,6$, agrees very well with the results of Pawley and co-workers,[6] $0.221\,654\pm0.000\,006$ and Blöte and co-workers,[7,8] $0.221\,652\pm0.000\,006$ as well as the estimate from Adler[35] $0.221\,655\pm0.000\,005$. Our value for K_c appears, however, to be inconsistent with the estimate from Alves, Berg, and Villanova,[18] $0.221\,57\pm0.000\,03$ and those of Liu and Fisher,[9] $0.221\,620\pm0.00\,006$ and $0.221\,637\pm0.000\,006$.

Above we expressed some concern for the validity of the results for $|m|$. In fact, the value of K_c estimated from the maximum slope of $|m|$ differs substantially from that obtained from the other quantities, although it does agree within 2 standard deviation units. If we remove the $|m|$ result from the analysis, our estimate for K_c drops to $0.221\,657\,6\pm0.000\,002\,2$ which is in even better agreement with the other estimates presented above.

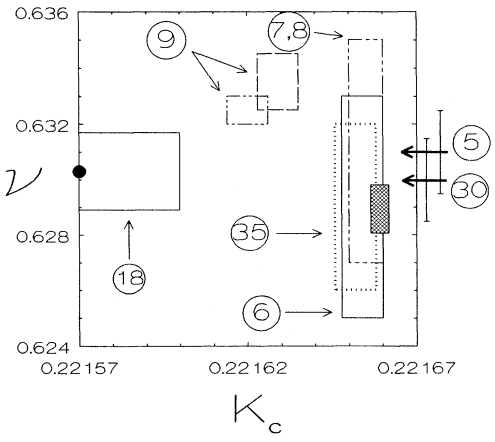

FIG. 8. High-resolution estimates for K_c and ν obtained using different methods. The arrows at the top show values for ν obtained from renormalization group and ϵ-expansion calculations which do not yield estimates for K_c.

V. CONCLUSIONS

The combination of high-statistics MC simulations of large systems, careful selection of measured quantities, and judicious use of histogram techniques can already produce results comparable to, or better than, those obtained by MCRG and series and ϵ expansion. Corrections to scaling can be included in the fits to help improve the accuracy in determining the dominant singularity but the data are not yet sufficiently accurate to allow us to study the corrections themselves. All of the analysis techniques used here are applicable if yet higher quality data are obtained, and should lead to results of truly unprecedented accuracy. It should be possible to obtain such data using recently developed techniques which avoid critical slowing down at least to a substantial extent. In order to improve upon our present analysis it will be necessary to obtain substantially better data for some of the large lattice sizes considered *and* to obtain high-quality data for substantially larger lattices. In addition, since different thermodynamic derivatives have peaks at different temperatures, multiple simulations are needed for each lattice size if we are to carry out an op-

timal extrapolation of effective critical temperatures to the thermodynamic limit for more than one quantity. Such calculations will be quite demanding of both computer memory as well as CPU time and are thus not trivial in scope.

ACKNOWLEDGMENTS

We are indebted to K. Binder and M. E. Fisher for helpful comments and suggestions. This research was supported in part by NSF Grant No. DMR-8715740.

[1]C. Domb, Adv. Phys. **9**, 149 (1960).
[2]M. E. Fisher, Rep. Prog. Phys. **30**, 615 (1967).
[3]B. G. Nickel, in *Phase Transitions: Cargèse 1980,* edited by M. Levy, J.-C. Le Guillou, and J. Zinn-Justin (Plenum, New York, 1982), p. 291.
[4]E. Brezin, J.-C. Le Guillou, and J. Zinn-Justin, Phys. Lett. **47A**, 285 (1974).
[5]J.-C. Le Guillou and J. Zinn-Justin, Phys. Rev. B **21**, 3976 (1980); J. Phys. (Paris) **48**, 19 (1987).
[6]G. S. Pawley, R. H. Swendsen, D. J. Wallace, and K. G. Wilson, Phys. Rev. B **29**, 4030 (1984).
[7]H. W. J. Blöte, J. de Bruin, A. Compagner, J. H. Croockewit, Y. T. J. C. Fonk, J. R. Heringa, A. Hoogland, and A. L. van Willigen, Europhys. Lett. **10**, 105 (1989).
[8]H. W. J. Blöte, A. Compagner, J. H. Croockewit, Y. T. J. C. Fonk, J. R. Heringa, A. Hoogland, T. S. Smit, and A. L. van Willigen, Physica A **161**, 1 (1989).
[9]A. J. Liu and M. E. Fisher, Physica A **165**, 35 (1989).
[10]D. P. Landau, Phys. Rev. B **14**, 255 (1976).
[11]M. N. Barber, R. B. Pearson, D. Toussaint, and J. L. Richardson, Phys. Rev. B **32**, 1720 (1985).
[12]G. Parisi and F. Rapuano, Phys. Lett. **157B**, 301 (1985).
[13]A. Hoogland, A. Compagner, and H. W. J. Blöte, Physica A **132**, 593 (1985).
[14]G. Bhanot, D. Duke, and R. Salvador, Phys. Rev. B **33**, 7841 (1986).
[15]M. Falcioni, E. Marinari, M. L. Paciello, G. Parisi, and B. Taglienti, Phys. Lett. **108B**, 331 (1982); E. Marinari, Nucl. Phys. **B235**, 123 (1984).
[16]G. Bhanot, K. Bitar, S. Black, P. Carter, and R. Salvador, Phys. Lett. B **183**, 331 (1987); **187**, 187 (1987); G. Bhanot, K. Bitar, and R. Salvador, *ibid.* **188**, 246 (1987).
[17]A. M. Ferrenberg and R. H. Swendsen, Phys. Rev. Lett. **61**, 2635 (1988); **63**, 1195 (1989); A. M. Ferrenberg and R. H. Swendsen, Comput. Phys. **3**, No. 5, (1989); A. M. Ferrenberg, in *Computer Simulation Studies in Condensed Matter Physics III,* edited by D. P. Landau, K. K. Mon, and H.-B. Schüttler (Springer-Verlag, Heidelberg, 1991).
[18]N. A. Alves, B. A. Berg, and R. Villanova, Phys. Rev. B **41**, 383 (1990).
[19]S. Wansleben, Comput. Phys. Commun. **43**, 315 (1987).
[20]R. C. Tausworthe, Math. Comput. **19**, 201 (1965).
[21]S. Kirkpatrick and E. Stoll, J. Comput. Phys. **40**, 517 (1981).
[22]S. Wansleben and D. P. Landau, J. Appl. Phys. **61**, 3968 (1987); Phys. Rev. B **43**, 6006 (1991).
[23]E. P. Münger and M. A. Novotny, Phys. Rev. B **43**, 5773 (1991).
[24]A. M. Ferrenberg, D. P. Landau, and K. Binder, J. Stat. Phys. **63**, 867 (1991).
[25]M. E. Fisher, in *Critical Phenomena,* edited by M. S. Green (Academic, New York, 1971).
[26]M. E. Fisher and M. N. Barber, Phys. Rev. Lett. **28**, 1516 (1972).
[27]M. N. Barber, in *Phase Transitions and Critical Phenomena,* edited by C. Domb and J. Lebowitz (Academic, New York, 1983), Vol. 8; V. Privman (editor), *Finite-Size Scaling and Numerical Simulation* (World Scientific, Singapore, 1990).
[28]F. J. Wegner, Phys. Rev. B **5**, 4529 (1972).
[29]A. Aharony and M. E. Fisher, Phys. Rev. B **27**, 4394 (1983).
[30]B. G. Nickel and J. J. Rehr, J. Stat. Phys. **61**, 11 (1990).
[31]A discussion of corrections to scaling for three-dimensional Ising models can be found in A. Liu and M. E. Fisher, J. Stat. Phys. **58**, 431 (1990).
[32]K. Binder, Z. Phys. B **43**, 119 (1981).
[33]M. E. Fisher, private communication.
[34]K. Binder, private communication.
[35]J. Adler, J. Phys. A **16**, 3585 (1983).
[36]M. P. Nightingale and H. W. J. Blöte, Phys. Rev. Lett. **60**, 1662 (1988).
[37]M. A. Novotny, Nucl. Phys. B: Lattice '90 supplement (to be published).